Vertical and Horizontal Seismic Impedance Moments, and Corner Frequencies

H.V.P. Truong
Research Engineer, Westminster Ca 92683, USA

SUMMARY:
Magnitudes of the current seismic moment have been modified by taking into account of mass density and Poisson's ratio of the rock layers based on the expressions of vertical and horizontal dynamic rock masses, and the dip angle of earthquake fault. The vertical magnitude of the seismic impedance moment has been defined as the ratio of the seismic moment and shear velocity of the rock layer. The ratio of the vertical and horizontal seismic impedance moments increases with the increase in the Poisson's ratio. The new expressions of vertical and horizontal magnitudes of seismic impedance moments and corner frequencies have also been presented and compared with the magnitudes of the current seismic moments and corner frequencies.

Keywords: Seismic Moment, magnitude, Poisson's ratio, impedance, shear modulus, density

1. INTRODUCTION

Several earthquake magnitude scales have been developed by seismologists, e.g. local magnitude M_L, surface-wave magnitude M_s, body-wave magnitude m_b, seismic moment M_o, and moment magnitude M_w. M_s and m_b estimates are usually different for a given earthquake, because m_b and M_s measure the amplitude of the P-wave and that of the surface wave, respectively. A problem with body and surface wave magnitudes is that they saturate or remain constant once earthquakes exceed a certain size. This happens because the added energy release in the very large earthquakes is all at longer periods than are measured by the 20 sec period surface waves. No matter how big an earthquake is, its body and surface wave magnitudes do not get above about 6.5 and 8.5, respectively. Hence for very large earthquakes these magnitude measurements underestimate the earthquake's size. The most commonly used scale today is the moment magnitude (M_w) scale. Moment magnitude is related to the physical size of fault rupture and the movement (displacement) across the fault, and as such is a more uniform measure of the strength of an earthquake. But, the current moment magnitude did not take into account of density, dip angle of the earthquake fault, and Poisson's ratio of the rock medium. Other consideration is that an earthquake normally has two components, i.e. vertical and horizontal components.

There are many uncertainties in estimating earthquake source parameters, such as stress drop, seismic moment and corner frequency, from single station measurements, so the idea of jackknife variance combined with a multitaper spectrum estimation to obtain confidence regions was used by Prieto et al. (2007) in order to obtain confidence intervals. Earthquake source parameter estimates have considerable uncertainties for several reasons: (i) Uncertainties due to earth's variability and deviations from the mathematical simplifications (ii) Uncertainties for historic earthquakes are large. Fault length estimates for the San Francisco earthquake vary from 300-500 km, Ms was estimated at 8.3 but now thought to be ~7.8, and fault width is essentially unknown and inferred from the depths of more recent earthquakes and geodetic data, and (iii) Fault dimensions and dislocations shown are average values for quantities that can vary significantly along the fault. Hence different studies yield varying and sometimes inconsistent values. Even so, data are sufficient to show effects of interest. Finally, for the same kind of earthquake magnitude, e.g. moment magnitude; different organizations or research

institutions have estimated with different values due to using different data sets for analyses, concepts, theories, and/or various methods, etc., e.g. the long period normal modes.

This paper proposes the new expressions of vertical and horizontal magnitudes of seismic impedance moments based on the expressions of the vertical and horizontal dynamic rock masses, and vertical and horizontal impedance-corner frequencies. Sensitivity analyses are also carried out on some earthquake source parameters, such as shear-wave velocity and dip angle of earthquake faults.

2. SEISMIC IMPEDANCE MOMENTS

One particularly useful alternative to Richter magnitude is the moment magnitude scale (M_w). Moment magnitude is based on the seismic moment of an earthquake, which is a direct measurement or estimate of the energy released by the earthquake. Seismic moment (M_o) can be calculated as follows:

$$M_o = RDA \tag{2.1}$$

Where R = rigidity of the material surrounding the fault, or shear modulus G of the crust or rock layer, D = the average displacement on the fault during the earthquake, and A = the total area of rupture on the fault.

Seismologists often favor using the seismic moment because it is the most physically-based estimate of the earthquake energy. Seismic moment can be converted into a magnitude scale using the following equation (Hank and Kanamori, 1979).

$$M_w = \frac{2}{3}\log M_o - 10.7 \tag{2.2}$$

Where M_o = seismic moment in Dyne-cm.

The concept of mantle magnitude M_m, introduced initially for Rayleigh waves and later extended to Love waves (Okal and Talandier, 1989, and 1990), is an attempt to define a magnitude scale firmly related to seismic moment M_o (and in particular to avoiding the well-known saturation effects suffered by M_s and other scales defined at constant periods), while at the same time retaining the basic philosophy of a magnitude scale, i.e., a quick, one station measurement that does not require the knowledge of either the earthquake's focal geometry, or its exact depth (Okal, 1992). Mm determinations were extensively verified and are said to be accurate by about ± 0.2 magnitude units (Hyvernaud et al., 1993).

$$M_m = \log M_o - c \tag{2.3}$$

Where c = 20 and 13 for the values of Mo given in dyne-cm and Newton-m, respectively.

The expressions of the vertical and horizontal dynamic rock masses (**DRMs**) for earthquakes based on the vertical and horizontal dynamic soil masses (**DSMs**) from the theory of wave propagation in soils (Truong, 2009, 2010, 2011a and b) have been defined, respectively, as

$$m_{zr} = \frac{A\sqrt{\rho_r G_r}}{\omega_z s_r} \tag{2.4}$$

$$m_{xr} = \frac{A\sqrt{\rho_r G_r}}{\omega_x} \tag{2.5}$$

Where ρ_r = Mass Density of the rock layer, G_r = Shear Modulus of the rock layer and

$$s_r = \frac{\sqrt{(1-2\mu_r)}}{\sqrt{2(1-\mu_r)}} \tag{2.6}$$

Where μ_r = Poisson's ratio of the rock.

The vertical and horizontal dynamic rock masses were originated by the vertical and horizontal components of an earthquake, respectively. If the earthquake has no vertical component, then the vertical dynamic rock mass (DRM) is equal to zero. The rigidity of the material surrounding the fault should have not only the shear modulus, but also the mass density of the material, as derived from the theory of wave propagation in soil or rock layers.

In the expressions of dynamic rock masses, the impedance factor, or rigidity of the medium, is normally defined as the square root of the product of shear modulus and mass density by many researchers. For example, Boore et al. (1997) have used the impedance factors of rock and soil layers to define the amplification factors for soft soil layers. The additional terms, mass density, dip angle of the earthquake fault, and Poisson's ratio could contribute to localize the moment magnitudes for site conditions, as also mentioned by Drouet et al. (2010) to study for local earthquake magnitudes in France. The vertical and horizontal seismic impedance moments with the use of the impedance factors can be defined based on the expressions of vertical and horizontal dynamic rock masses (Truong, 2009, 2010, 2011a and b), and the dip angle of the earthquake fault, as follows:

$$M_{ioz} = \frac{DA\sqrt{G\rho}}{s_r}\sin\theta = \frac{M_0 \sin\theta}{V_s s_r} \tag{2.7}$$

$$M_{iox} = DA\sqrt{G\rho}\cos\theta = \frac{M_o \cos\theta}{V_s} \tag{2.8}$$

Where θ = Dip angle of earthquake faults, e.g. 25-30^o for thrust earthquakes.

The ratio of the vertical and horizontal seismic impedance moments depends on the Poisson's ratio of the rock medium, and increases with the increase in the Poisson's ratio of the rock medium and the dip tangle, as

$$R_{izx} = \frac{M_{ioz}}{M_{iox}} = \frac{\sin\theta}{s_r \cos\theta} = \frac{\tan\theta}{s_r} \tag{2.9}$$

3. VERTICAL AND HORIZONTAL IMPEDANCE-MOMENT MAGNITUDES

The vertical and horizontal impedance-moment magnitudes based on the vertical and horizontal seismic impedance moments can be proposed for, respectively, as:

$$M_{iwz} = \frac{2}{3}\log M_{ioz} - c \tag{3.1}$$

$$M_{iwx} = \frac{2}{3}\log M_{iox} - c \tag{3.2}$$

Where M_{io} = seismic impedance moment in Dyne-cm or in N-m dependent on constant c, c = constant and equal to 6.7 for M_{io} in Dyne-cm, and 3.4 for M_{io} in N-m, respectively.

The values of the vertical and horizontal impedance-moment magnitudes must be comparable with the current values of the other magnitudes, e.g. moment magnitude M_w, local magnitude M_L and surface-wave magnitude Ms, etc., but also improve the localization with the site conditions. The effects of impedance factors on moment magnitudes based on the velocity of Rayleigh wave can be estimated by replacing the shear wave velocity by Rayleigh-wave velocity in Eqns. (3.1) and (3.2). The value of the Rayleigh-wave velocity, V_R can be determined from the shear wave velocity (Richart et al., 1970) by:

$$V_R = kV_s \tag{3.3}$$

Where k is determined by

$$k^6 - 8k^4 + (24 - 16s^2)k^2 + 16(s^2 - 1) = 0 \tag{3.4}$$

The particle motion associated with the compressive wave is push-pull motion parallel to the direction of the wave front; the particle motion associated with the shear wave is a traverse displacement normal to the direction of the wave front; and the particle motion associated with the Rayleigh wave is made up two components (horizontal and vertical) which vary with depth (Richart et al., 1970). The impedance-moment magnitude based on the Rayleigh-wave velocity, which can be defined as the impedance-mantle magnitude, can be proposed as follows:

$$M_{im} = \frac{2}{3}\log M_{iox} - 3.5 \tag{3.5}$$

Where M_{iox} = horizontal seismic impedance moment in N-m.

The value obtained from Eqn. (3.5) could be used to compare with the mantle magnitude M_m (Okal and Talandier, 1989, and 1990). The effects of impedance factors on moment magnitudes based on the velocity of Love wave can be estimated by replacing the shear wave velocity with Love-wave velocity in Eqns. (3.12) and (3.2). Love wave consists of a horizontally polarised shear wave. Ewing et al. (1957) described the Love wave as a horizontally shear wave trapped in a superficial layer and propagated by multiple reflections.

For the 2004 Indian Ocean megathrust earthquake, the seismic moment is 4.0×10^{22} Newton-m, the shear-wave velocity of the rock medium, the dip angle, and Poisson's ratio are assumed to be equal to 4000 m/s, 30^o, and 0.15, respectively; the moment magnitude based on the work by Hank and Kanamori (1979) (Eqn. (3.1)) and the mantle magnitude are 9.01 and 9.60, respectively. While, the horizontal and vertical impedance-moment magnitudes are 9.24 and 8.94, respectively (Table 3.1). The Pacific Tsunami Warning Center has accepted the moment magnitude of 9.0, The United States Geological Survey (USGS) has so far not changed its estimate of 9.1. The most recent studies in 2006 have obtained a magnitude between 9.1-9.3. Dr. Hiroo Kanamori of the California Institute of Technology believes that M_w 9.2 is a good representative value for the size of this great earthquake (Wikipedia – The Free Encyclopedia). From the long period normal modes, the seismic moment as large as 1.0×10^{30} Dyne-cm (moment magnitude M_w = 9.3) was estimated by Stein and Okal (2005 and 2007). The seismic moment, moment magnitude, mantle magnitude, the horizontal and vertical impedance magnitude, and the impedance-mantle magnitude increase with the increase in the shear modulus of the rock medium (Table 3.1 and Fig. 3.1). The fourth and fifth columns in Table 3.1 are the mantle magnitudes using the values of the shear-wave velocity and the Rayleigh-wave velocity,

respectively. The last column showed the values of impedance-mantle magnitudes using the Rayleigh-wave velocity. The lowest and highest values of the magnitudes are the moment magnitude and the mantle magnitude, as shown in columns 3 and 4, respectively.

Table 3.1. Variation of different magnitudes with the shear modulus of the rock medium

V_s (m/s)	M_o (x 10^{22})	M_w	M_m (V_s)	M_m (V_R)	M_{iox}	M_{ioz}	M_{im}(V_R)
4000	4.00	9.01	9.60	9.53	9.23	9.19	9.11
4500	5.06	9.08	9.70	9.62	9.26	9.23	9.14
5000	6.25	9.14	9.80	9.72	9.29	9.26	9.17
5500	7.56	9.19	9.88	9.81	9.32	9.29	9.20

For the megathrust earthquake such as the 2004 Sumatra earthquake, the value of the horizontal impedance-moment magnitude of 9.23 is higher than the vertical impedance-moment magnitude of 9.19, and the impedance-mantle magnitude of 9.11, because of the low dip angle of 30° or the higher seismic impedance moment. If the dip angle of 60° or for normal faults with the same seismic moment, the vertical impedance-moment will be 9.35 which is higher than the horizontal impedance-moment magnitude of 9.07 and the impedance-mantle magnitude of 8.95; because the P-wave velocity is higher than the S-wave velocity and the Rayleigh-wave velocity.

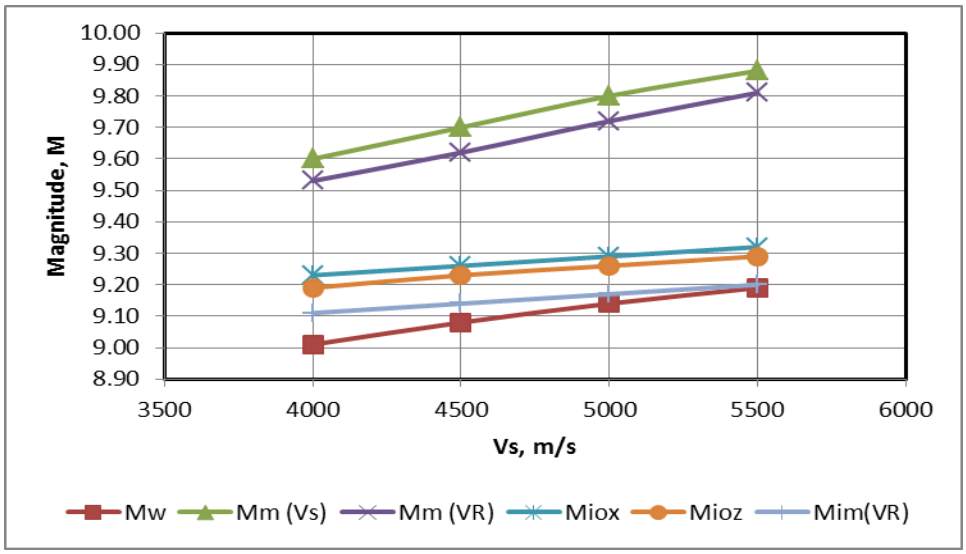

Figure 3.1. Variation of different magnitudes with the shear modulus of the rock medium

If the dip angle of the Sumatra earthquake decreases from 30° in Table 3.1 to 25° and 10°, respectively; the horizontal impedance-moment magnitude increases to 9.24 and 9.26, respectively; while the vertical impedance-moment magnitude decreases to 9.15 to 8.89, respectively.

4. RELATIONS BETWEEN SEISMIC IMPEDANCE MOMENT AND SURFACE-WAVE MAGNITUDE

The relationship between the seismic impedance moment and the surface-wave magnitude M_s based on the work by Ekstrom et al. (1988) and Chen et al. (1989) can be expressed as

$$M_S = \frac{2}{3}\log M_{iox} - 5.7 \qquad 8.5 \geq M_s \geq 5.3 \tag{4.1}$$

$$M_s = \log M_{iox} - 8.6 \qquad M_s \prec 5.3 \tag{4.2}$$

Where M_{iox} = value given in Newton-m.

The lower limit of 5.3 has been set by Ekstrom et al. (1988), and the upper limit set by Chen et al. (1989) in their expressions of relationships between the seismic moment and the surface-wave magnitude, respectively, are appearing in the right hand sides of Eqns. (4.1) and (4.2). Note that the strongest earthquake of the 20th century in 1960 Chile 1960 had a seismic moment M_o of about 3.10^{23} Nm and "a saturated" magnitude of Ms = 8.5. No Ms > 8.5 has ever been measured although moment magnitudes up to 9.5 to 10 have been observed. This effect is termed magnitude saturation. Using almost 400 events, Choy et al. (1995) derived the relationship for the seismic energy and the surface-wave magnitude as

$$\log E_s = 1.5M_s - 4.4 \tag{4.3}$$

5. IMPEDANCE-CORNER FREQUENCIES

The corner frequency of an earthquake has been defined by Joyner et al. (1988) as

$$f_c = 4.9(10)^6 V_s \left(\frac{\Delta\sigma}{M_o}\right)^{1/3} \tag{5.1}$$

Where V_s = Shear-wave velocity of the rock medium in km/s, $\Delta\sigma$ = earthquake stress drop in bars. Stress drop means the difference in acting stress at the source region before and after the earthquake.

The corner frequency is certainly related to the size of the earthquake source. According to Brune (1970) and Madariaga (1976), both of whom modelled a circular fault, the corner frequency in the P or S-wave spectrum, respectively, is

$$f_c = k\frac{V_s}{r} \tag{5.2}$$

Where k = model dependent constant; k = 0.32 for P-wave spectrum, and 0.21 for S-wave spectrum for the rupture velocity of $0.9V_s$ (Madariaga, 1976); and k =0.375 for S-wave spectrum (Brune, 1970). The corner frequency of S-wave spectrum by Madariaga (1976) is about a factor of two lower than that of Brune (1970). Madariaga (1976) also proposed the corner frequency based on the seismic moment and earthquake stress drop for circular fault, as

$$f_c = (kVs)\left(\frac{16\Delta\sigma}{7M_o}\right)^{1/3} \tag{5.3}$$

In contrast, assuming a rectangular fault, Haskell (1964) gives the relationships

$$f_c = c_m \frac{V_{p,s}}{(LW)^{1/2}} \tag{5.4}$$

Where c_m = model dependent constants, r = fault radius, L = Fault length, and W = fault width.

In general, the vertical and horizontal corner frequencies depend on the rupture velocity of the fault, the fault area, the coefficient of friction of the material surrounding the fault, and the dip angle of the fault plane to the plane of the maximum principle stress. Laboratory studies of rocks show that at the

depths typical of earthquakes, the coefficient of friction is from 0.6 to 0.85 for the majority of rocks (Byerlee, 1978). So, the fault should form at angles of 25-30^o to the maximum principle stress, they are optimally oriented. Because the principle stress is horizontal and vertical for thrust and normal fault, respectively; the angles between the faults and the horizontal surface (i.e. dip angles) should be about 25-30^o for thrust and 60-65^o for normal faults if they are optimally oriented (Kanamori et al. 2004). The vertical and horizontal corner frequencies based on the wave velocity, fault area and dip angle have been proposed, respectively, as.

$$f_{cz} = \frac{V_{rup}}{s(LW\sin\theta)^{1/2}} \tag{5.5}$$

$$f_{cx} = \frac{V_{rup}}{(LW\cos\theta)^{1/2}} \tag{5.6}$$

Where V_{rup} = Rupture velocity, e.g. to be 70-95% of the Shear-wave velocity for some shallow large earthquakes (Kanamori et al., 2004), and θ = Dip angle of the fault, e.g. 60-65^o for normal faults.

The vertical and horizontal impedance-corner frequencies based on the vertical and horizontal seismic impedance moments have been proposed as

$$f_{icz} = c_f (10)^5 \left(\frac{\Delta\sigma}{M_{ioz}} \right)^{1/3} \tag{5.7}$$

$$f_{icx} = c_f (10)^5 \left(\frac{\Delta\sigma}{M_{iox}} \right)^{1/3} \tag{5.8}$$

Where c_f = constants are equal to 1.9 and 4.1 when the values of M_{io} are in Dyne-cm and N-m, respectively.

The vertical and horizontal impedance-corner frequencies are also called the P-wave and S-wave corner frequencies, respectively (Molnar et al., 1973). For normal earthquakes, the horizontal impedance-corner frequency is slightly higher than the vertical impedance-corner frequency, because the vertical impedance-corner frequency has the higher vertical seismic impedance moment than that in the horizontal direction. Savage (1972) showed that for bilateral rupture, on the average, the S-wave corner frequency is slightly higher than P-wave corner frequency. Note that the ratio of P-wave velocity of propagation and the S-wave velocity of propagation is always greater than 1, and increases with the increase in the Poisson' s ratio of the rock medium (Richart et al., 1970). Bakun et al. (1976) have showed that the higher corner frequencies of S-wave spectra are higher than those of P-wave spectra for small earthquakes in central California. Several investigators have studied the relation between the corner frequencies of the S and P waves. Observations of small earthquakes (Mw $\leq$ 5) by Molnar et al. (1973) show that the P-wave corner frequencies are larger than the S-wave corner frequencies. The same conclusion was drawn from studies of large earthquakes recorded at teleseismic distances (Wyss and Hanks, 1972; Wyss and Molnar, 1972). However, determining corner frequencies is subject to large errors and is not reliable; moreover, many of these studies use data from a few stations and are hence not robust (Venkataran and Kanamori, 2004). The horizontal impedance-corner frequency, which is also dependent on the maximum slip velocity of earthquake (Anil-Bayrak et al., 2009), can be expressed in terms of the seismic moment or the horizontal seismic impedance moment as

$$f_{icx} = \frac{e}{2\pi}\frac{v_m \rho V_s^2 A}{M_0} = \frac{e}{2\pi}\frac{v_m \rho V_s A}{M_{iox}} \tag{5.9}$$

Where e = base of the natural logarithm (=2.71828), and v_m = maximum slip velocity of earthquake.

For the 1999 Chi-Chi Taiwan reverse (thrust) earthquake, the seismic moment is 2.4×10^{20} Newton-m (M_w = 7.6 by USGS), the shear-wave velocity of the rock medium, the dip angle, and Poisson's ratio are assumed to be equal to 3075 m/s, 30°, and 0.15, respectively; the moment magnitude based on the work by Hank and Kanamori (1979) (Eqn. (3.1)) and the mantle magnitude are 7.53 and 7.38, respectively. While, the horizontal and vertical impedance-moment magnitudes are 7.82 and 7.79, respectively (Table 5.1 and Figure 5.1).

Table 5.1. Variation of Different Magnitudes with Dip Angles

Dip Ang.	Mw	Mm	Micx	Micz	Mim	Ms E&C	Mim
60	7.53	7.38	7.66	7.95	7.54	7.49	7.26
30	7.53	7.38	**7.82**	**7.79**	7.70	7.49	7.42
20	7.53	7.38	7.84	7.68	7.73	7.49	7.44
10	7.53	7.38	7.86	7.48	7.74	7.49	7.46
5	7.53	7.38	7.86	7.28	7.74	7.49	7.46

The surface-wave magnitude based on the work by Ekstrom et al. (1988) and Chen et al. (1989) is constant with the dip angle, as shown as Ms E&C in Table 5.1 and Fig. 5.1; while the impedance moment magnitude using the Rayleigh-wave velocity increases with the increase in the dip angle of earthquake fault, as denoted as M_{im} in Table 5.1 and Fig. 5.1. The corner frequencies of the methods by Joyner et al. (1988), Brune (1970), and Madariaga (1976) are constants with the increase in dip angles; while the horizontal and vertical impedance-corner frequencies based on the lengths and stress drops vary with the dip angles (Table 5.2 and Fig. 5.2). For normal fault with dip angle of 30°, the vertical impedance-corner frequency is greater than that in the horizontal direction. The horizontal impedance-corner frequency decreases with the decrease in the dip angle of the earthquake faults. In general, the ratio of the vertical impedance-corner frequency to the horizontal impedance-corner frequency is always greater than; exceptionally, for case of the normal fault with the dip angle of 60° and the corner frequencies estimated by using the drop-stress method, the vertical impedance-corner frequency of 0.0541 is lower than the horizontal impedance-corner frequency of 0.0561 (Table 5.2 and Fig. 5.2).

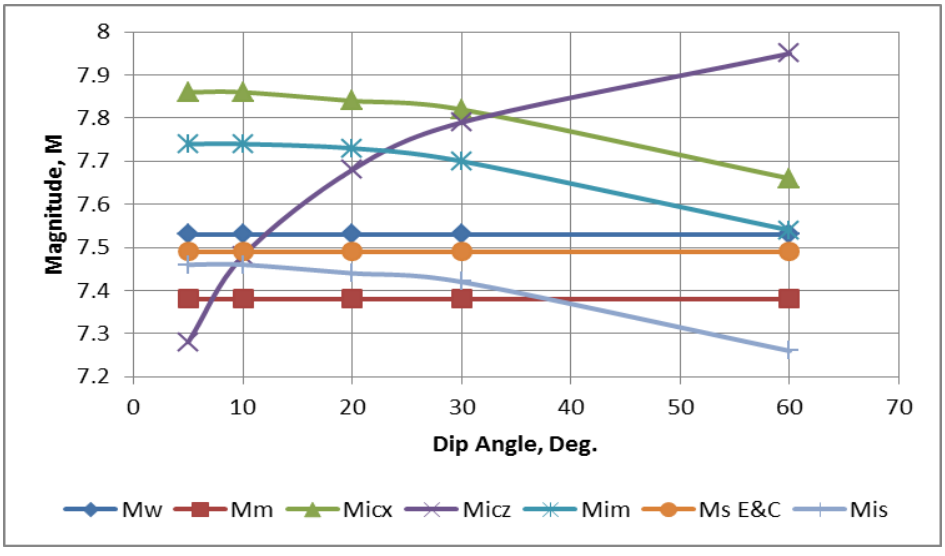

Figure 5.1. Variation of different magnitudes with dip angles

Table 5.2. Variation of Different Corner Frequencies with Dip Angles by Various Methods

Dip Ang.	fc	Brune	Mad x	Mad z	I x A	I z A	I x S	I z S
60	0.0522	0.0361	0.0202	0.0308	0.0692	0.082	**0.0561**	**0.0541**
30	0.0522	0.0361	0.0202	0.0308	0.0526	0.108	0.0467	0.0650
20	0.0522	0.0361	0.0202	0.0308	0.0505	0.130	0.0454	0.0738
10	0.0522	0.0361	0.0202	0.0308	0.0493	0.183	0.0447	0.0925
5	0.0522	0.0361	0.0202	0.0308	0.0490	0.258	0.0446	0.1165

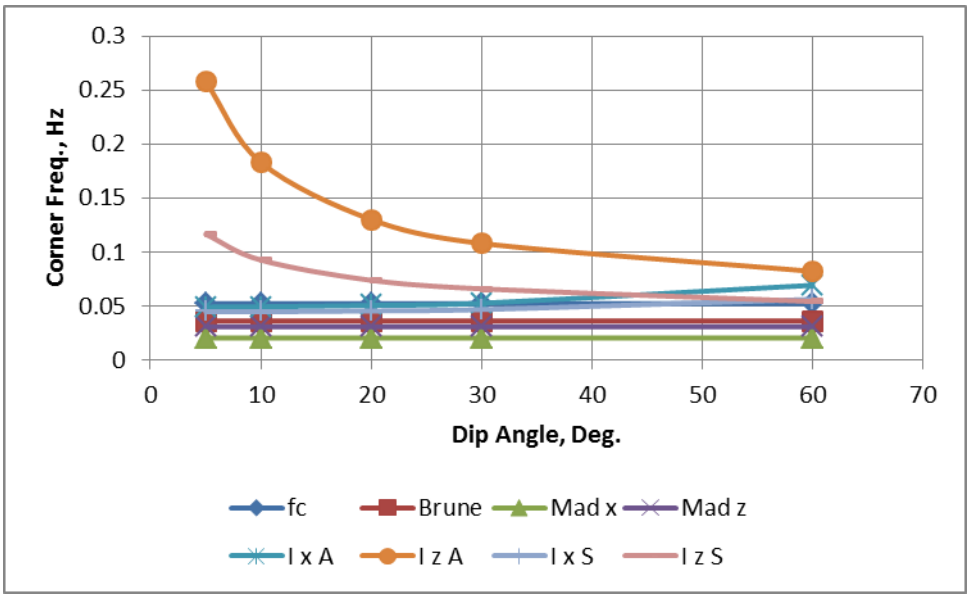

Figure 5.2. Variation of different corner frequencies with dip angles

6. CONCLUSIONS

For the thrust faults, the horizontal impedance-moment magnitude is higher than the vertical impedance-moment magnitude. The ratio of the vertical and horizontal impedance-moment magnitudes increases with the increase in the dip angle of earthquake fault and Poisson's ratio of the rock medium. The dip angle of earthquake fault must be taken into account in estimating seismic moment, moment magnitude, and corner frequencies in order to provide better the site conditions of the earthquake faults. The vertical impedance-corner frequency increases with the decrease in the dip angle, while the horizontal impedance-corner frequency decreases with the decrease in the dip angle of the earthquake faults.

In general, the P-wave corner frequencies are higher than the S-wave corner frequencies; especially, if the corner frequencies are estimated through the rupture velocities of the earthquake faults, as expected. For normal faults, e.g. the dip angle of 60^{o}, the S-wave corner frequency is higher than the P-wave frequency if the methods of stress drop are used.

REFERENCES

Anil-Bayrak, N.A. and Beresnev, I.G. (2009). Fault slip velocities inferred from the spectra of ground motions. . *Bulletin of the Seismological Society of America,*Vol.**99**, No**. 2A**, 876-883.

Bakun, W.H., Bufe, C.G. and Stewart, R.M. (1976). Body-wave spectra of central California earthquakes. *Bulletin of the Seismological Society of America,*Vol.**66**, 363-384.

Boore, D.M. and Joyner, W.B. (1997). Site Amplifications for Generic Rock Sites. *Bulletin of the Seismological*

Society of America, **Vol.87, No.2**, 327-341.
Brune, J.N. (1970). Tectonic stress and the spectra of seismic shear waves from the earthquakes. *J. Geophys. Res.,* Vol.**75**, 4997-5009.
Byerlee, J. (1978). Friction of rock. *Pure Appl. Geophys.*, **116,** 615-626.
Chen, P. and Chen. H. Sacling law and its applications to earthquake statistical relations. *Techotonophysics.***166,** 53-72.
Choy, G.L. and Boatwright, J. (1995). GLoal patterns of radiated by shallow earthquakes. *J. Geophys. Res.*,**91, 18**, 18205-18288.
Drouet, S., Cotton, F. and Gueguen, P. (2010). V_{s30}, K, regional attenuation and M_w from accelerograms: application to magnitude 3-5 French earthquakes. *Geophys. J. Int.,* **182,** 80-898.
Ekstrom, G. and Dziewonski, A.M. (1988). Evidence of bias in estimations of earthquake size, *Nature,* **332,** 319-323.
Ewing, W.M., Jardetzky, W.S. and Press, F. (1957). Elastic Waves in Layered Media. McGrawHill Book Co. (New York), 380 p.
Hanks, T. C. and Kanamori, H. (1979). A Moment Magnitude Scale. *J. of Geophysical Research*, Vol. **84**, No.**B5**, 2348-2350.
Haskell, N.A. (1964). Total energy spectral density of elastic wave radiation from propagating faults. *Bulletin of the Seismological Society of America,***54, No.6**, 1811-1841.
Hyvernaud, O., Reymond, D., Talandier, J. and Okal, E.A. (1993). Four years of automated measurement of seismic moments att Papeete using the mantle mangitude Mm:1987-1991. *Tectonophysics,* **217**,175-193.
Joyner, W.B. and Boore, D.M. (1988). Measurement, Characterization, and prediction of strong ground motion. *Reprinted from Proc. Earthquake Eng. And Soil Dynamics II*, GT Div/ASCE.., Park City, Utah, 60 p.
Kanamori, H. and Brodsky, E.E. (2004). The physics of eathquakes. *Reports on Progress in Physics.***67,** 1429-1496.
Madariaga, R. (1976). Dynamics of an expanding circular fault. *Bulletin of the Seismological Society of America,***66**, 639-667.
Molnar, P., Tucker, B.E. and Brune, J.N. (1973). Corner frequencies of P and S waves and Models of earthquake sources. *Bulletin of the Seismological Society of America,***63**, 2091-2104.
Okal, E.A. (1989). A theoretical discussion of time-domain magnitudes: the Prague Formula for M_s and the Mantle Mangitude M_m. *J. Geophys. Res.*, **94**, 4194-4204.
Okal, E.A. and Talandier, J. (1990). M_m : Extension to Love Waves of the concept of a Variable-method Mantle Magnitude. *Pure and Appl. Goephys.,* **134**, 355-384.
Okal, E.A. (1992). Use of Mantle Magnitude M_m for the Reassessment of the seismic moment of historical earthquakes, II. Intermediate and deep events. *Pure and Appl. Goephys.*, **139**, 17-57.
Prieto, G.A, Thomson, D.J., Vernon, F.L., Shearer, P.M. and Parker, R.L. (200&0. Confidence intervals for earthquake source parameters. *Geophys. J. Int*, **168**, 1227-1234.
Richart, F.E. Jr., Woods, R.D., and Hall, J.R. (1970). Vibrations of Soils and Foundations. *Prentice-Hall,* 414p.
Savage, J.C. (1972). Relation of corner frequency to fault dimensions. *J. Geophys. Res.***77,** 3788-3795.
Stein, S. and Okal, E.A. (2005). Speed and size of the Sumatra earthquake. *Brief Communications. Nature,* **434,** 581-582.
Stein, S. and Okal, E.A. (2007). Ultralong period seismic study of the December 2004 Indian Earthquake and implications for regional techntonics and the subduction process. *Bulletin of the Seismological Society of America,***Vol. 97, No.1A,** s279-s295.
Truong, H.V.P. (2009). "Added Soil Mass and Ratio of Damping For Vertical and Horizontal Vibration", *Proc.11thConference on Science and Technology*, University of Technology in Saigon, Vietnam National University, Vietnam: 24-30.
Truong, H.V.P. (2010), "Effects of Damping and Dynamic Soil Mass on Footing Vibration' *Proc. GeoShanghai International Conference* in Shanghai in June 2010 (ASCE -GSPs), 177-183.
Truong, H.V.P. (2011a) "Dynamic Soil Mass and Resonant Frequency of Pile Foundations" *Proc. 14th Asian Regional Conference on Soil Mechanics and Geotechnical Engineering*, 23-27 May 2011, Hong Kong, Paper No.332.
Truong, H.V.P. (2011b). Dynamic Soil Mass or Added Soil Mass and Dynamic Rock Mass in Foundation Designs and Dynamic Soil Amplification. *Proc. of World Congress on Advances in Structural Engineering and Mechanics (ASEM+)*, Korea: 4893-4901.
Venkataraman, A and Kanamori, H. (2004). Effect of directivity on estimates of radiated seismic energy. *Journal of Geophysical Research,* Vol.**109**, B04301, 12 p.
Wyss, M. and Hanks, T. (1972). The source parameters of the San Fernandao earthquake (February 9, 1971) inferred from teleseismic body waves. *Bulletin of the Seismological Society of America,* **62**, 591-602.
Wyss, M. and Molnar, P. (1972). Source parameters of intermediate and deep focus earthquakes in the Tonga Arc. *Earth Planet Inter.*,**6,** 279-292.